Direct detection of organophosphate compounds in water by a fluorescence-based biosensing device

Paola Carullo[1§], Marco Chino[2§], Giovanni Paolo Cetrangolo[1], Sara Terreri[3], Angela Lombardi[2], Giuseppe Manco[1], Amelia Cimmino[3]*, Ferdinando Febbraio[1]*

[1]Institute of Protein Biochemistry – CNR. Via P. Castellino 111, 80131 – Naples, Italy;
[2]Department of Chemical Sciences, - University of Naples "Federico II". Via Cintia, 80126 Napoli, Italy
[3]Institute of Genetics and Biophysics "Adriano Buzzati Traverso",– CNR. Via P. Castellino 111, 80131 – Naples, Italy;

p.carullo@ibp.cnr.it, marco.chino@unina.it, g.cetrangolo@ibp.cnr.it, sara.terreri@igb.cnr.it, alombard@unina.it, g.manco@ibp.cnr.it, amelia.cimmino@igb.cnr.it, f.febbraio@ibp.cnr.it.

§ These authors contributed equally to this work.
* Correspondence: f.febbraio@ibp.cnr.it; Tel.: +39-081-613-2611, amelia.cimmino@igb.cnr.it Tel.: +39-081-613-2304

Abstract: The main drawbacks in the use of acetylcholinesterase-based biosensors are their susceptibility to inhibition by too many chemicals, their limited time-stability, and the constant need for a supply of substrates for the measurements. In order to offset these deficiencies, we have addressed our studies towards the thermophilic esterase 2 from *A. acidocaldarious*, which shows a high specificity and affinity towards organophosphates and a high resistance under raw operative conditions. In particular, we have investigated the possibility of measuring the binding of organophosphates to the protein by using a fluorescent probe covalently linked near the active site. We have produced a mutant where the serine 35, a residue located at the entrance of the alcohol binding site, has been replaced by a cysteine residue. The addition of 1,5-IAEDANS as a fluorescent probe to the thiol group of the mutant-protein did not affect the capability of the enzyme to bind the paraoxon and its stability or instability over time. We have set up a continuous flow system based on a re-circulating solution of the probe-enzyme complex through a fluorimetric flow cell inside a spectrofluorimeter. The addition of paraoxon aliquots has been detected in real-time by measuring the fluorescence quenching of the probe-enzyme complex. The fluorescence signals, as well as the enzyme activity, were not affected by dilution and organic solvent addition. These results support the development of biosensing devices for the continuous monitoring of organophosphate compounds.

Keywords: biosensing device; thermophilic esterase; fluorescent probe; organophosphates; flow cell.

1. Introduction

Organophosphate (OP) compounds are esters of phosphoric acid, which is the basic building block of many neurotoxic compounds, such as insecticides and nerve agents [1,2]. It acts by means of an irreversible inactivation of acetylcholinesterase (AChE), a key enzyme for nerve functions in insects, humans, and many other animals [3]. For this reason, AChE-based enzymatic biosensors have been reported in literature to be the most promising tool for OP detection in order to control toxicity and for the preservation of the environment. However, not only phosphates but also phosphonates, phosphinates, as well as some other derivatives like fluoroanhydrides of organophosphoric acids, exert irreversible inhibition on the AChE, making difficult the determination of specific pesticides, so become necessary further studies to developing appropriate bioreceptors.

The different types of biosensors based on AChE inhibition introduced since 1993 differ in the type

of support and technique utilized for the immobilization of the enzyme. In addition, they are also classified according to the type of system used for the signal transduction (electrochemical, optical, potentiometric or amperometric) [4]. Recent developments include the use of AChE in combination with functional nanoscaffolds made of novel nanomaterials, such as metal and metal oxide nanoparticles, quantum dots (QDs), and magnetic beads for the optical detection of pesticides [5–7]. Representative detection limits of AChE based biosensors are in the range from 10^{-11} to 10^{-17} M [8], evidencing a very high sensitivity with respect to the results obtained by using conventional GC/MS methods (0.5×10^{-9} M). More recent research has demonstrated very sensitive limits of detection (LOD) of 10^{-14} M and 10^{-12} M for the detection of paraoxon and dichlorvos obtained with a photoelectrochemical (PEC) biosensor with AChE as the biorecognition element [9].

Despite the interesting data that show their good sensitivity for detection purposes, AChE based biosensors still have significant limitations. First, they require the presence of an acetylcholine-like substrate to measure the variation of AChE residual activity after OP irreversible inhibition. Secondly, this type of biosensor shows a poor selectivity in multicomposite mixtures and complex matrices. Thirdly, it is not suitable for the identification of a specific pesticide. In addition, the intrinsic low stability over time of AChE makes this type of biosensor not suitable to use for real-time or continuous biosensing in the field, like traditional systems of analysis such as LC- and GC-MS.

The awareness of these limitations has resulted in the search for new enzymes to use as the bioreceptor parts in a biosensor. The use of a thermostable carboxylesterase from *A. acidocaldarious* (EST2) involves some significant advantages compared to the use of enzymes such as AChE.

EST2 is highly sensitive to the action of paraoxon, and appears to be endowed with a high affinity toward this OP pesticide [10]. Although paraoxon is not more used as a pesticide because considered dangerous for human health and for the environment, is still present in the environment being a metabolite of parathion [11] (Angelini et al., 2015), and stored as obsolete pesticide in third world countries. In addition, EST2 remarkable stability over time in a wide range of temperatures and pH and in aqueous and organic solutions (liquid foods) [12] supports its possible use in biosensing devices for the selective detection of OPs.

For the purpose of developing a biosensing device for the continuous and real-time detection of OPs, we have focused our efforts on the use of a stable enzyme, such as EST2, in combination with a very sensitive technique, such as fluorescence spectroscopy, and the integration of this approach with a system for the continuous measurement of a signal. We have already introduced the use of intrinsic fluorescence (of tryptophan) for the detection of OP binding to EST2 [13] but the use of UV wavelengths in complex solutions, such as liquid foods, has so far been limited. Therefore, we have produced an EST2 mutant where the serine 35 has been replaced by a cysteine residue (EST2-S35C), for the binding with a fluorescent probe, to use in visible fluorescence-based measurements for the real-time monitoring of neurotoxic compounds. In addition, we have tested the toxicity of our bioreceptor in a living cell culture in order to demonstrate the safety of this system in environmental detection.

2. Materials and Methods

2.1. Chemicals and Reagents

All reagents were of analytical grade and obtained from commercial sources. p-Nitrophenyl (p-NP) esters, Tri-n-butylphosphine (TBP), Diethyl-p-nitrophenyl phosphate (paraoxon) and ATTO 465 maleimide (ATTO465) were purchased from Sigma Chemical Co. (St. Louis, MO). 1,5-IAEDANS was purchased from Molecular Probe (Thermo Fisher Scientific, USA).

2.2. Computational analysis

The computer simulations for mutant design were carried out on the EST2 3D crystallographic structure resolved at 2.6 Å (ID number 1EQV from Protein Data Bank [http://www.rcsb.org/pdb/]) using the software Swiss PdbViewer version 3.7 [14]. The pdb file was opportunely edited to remove the HEPES group from the catalytic site, where it was covalently bonded to the Ser155 during the crystallization process. The residues in the neighborhood of the catalytic entrance were inspected in order to find a site for the binding to the fluorescent probes. The *in silico* mutations were carried out using the in-built mutation tools of the Swiss PdbViewer, and the energy minimization performed with the partial implementation of the GROMOS96 force-field. The values of the intramolecular distances between the side chains of the aminoacid residues after mutation were calculated.

2.3. Cloning, over-expression and purification of EST2-S35C in E. coli

The plasmid containing the synthetic gene with a point mutation of a serine residue with a cysteine residue in position 35 was purchased from GeneArt - Life Technologies (Regensbur-Germany). The fragment was cloned into a pET41b(+)_K430 plasmid using the Ndel and Sac1 cloning sites. The final construct was verified by sequencing.

EST2-S35C was over-expressed in the mesophilic host *E. coli* strain BL21 (DE3) and purified as previously described in Manco et al. [15], with slight modifications (see Supplementary Materials for details). The principal modification of Manco's purification protocol concerned the use of Tributylphosphine (TBP), an uncharged reducing agent, in the buffer solution for each purification step. TBP acts as a weak base in organic solvents and it is an important catalyst for the acylation reactions [16]. It does not interfere with the modifications of cysteines with alkylating agents unlike other reducing agents with a different nucleophilicity [17]. The yield in the biomass was comparable with that described for wild type enzyme in Manco et al. [15]. The purity of the enzymatic solution was tested by SDS-PAGE (single band obtained). The protein concentration was estimated with the optical absorbance at 280 nm, using a molar extinction coefficient of 1.34×10^5 M^{-1} cm^{-1} in 25 mM Tris/HCl buffer, pH 8.5, containing 0.5 mM EDTA and 1 mM TBP at 25 °C. The protein concentration was also determined using the Bio-Rad dye reagent (BIO-RAD – USA) with bovine γ-globulin as standard, according to the Bradford method [18].

2.4. Enzyme assays

A standard assay was carried out by monitoring the production of p-nitrophenoxide from the hydrolysis of p-NP esters at the wavelength of 405 nm in 1 cm path-length cells with a double-beam Varian Cary1E UV–visible spectrophotometer equipped with a temperature controller based on Peltier heat-exchange devices. The standard assay contained 0.2 mM p-NP-exanoate in 40 mM Na_2HPO_4/NaH_3PO_4, pH 7.1, and 2% (v/v) Triton X-100. Enzyme characterization was carried out over the temperature range 30–70 °C. A reference sample without the enzyme was used to subtract the background hydrolysis of the substrate. Kinetic constants on p-NP-exanoate were determined by measuring the enzymatic activity in the standard condition at substrate concentrations in the range from 5 to 180 μ*M*. The kinetic constant values (K_M and k_{cat}) were calculated by plotting the reciprocals of EST2 hydrolysis rates *versus* the substrate concentrations (Lineweaver-Burk transformation plot). All measures were carried out at least three times, and the data were analyzed

by the software QtiPlot 0.9.8.9 (Copyright 2004 - 2011 Ion Vasilief).
One unit of enzymatic activity was defined as the amount of protein releasing 1 μmol of p-nitrophenoxide/min from the p-NP ester at the indicated temperature.

2.5. Inhibition assay
Aliquots of the enzyme (2.1 x 10^{-12} moles) were incubated in 25 mM Tris/HCl, pH 7.4, at RT, in the presence of increasing concentrations of paraoxon in the range from 0.05 to 0.2 x 10^{-9} M. The reactions were monitored, following the residual enzymatic activity, by assaying sample aliquots at different times, as described in the standard assay.

2.6. Binding probe-enzyme: Sample preparation and conjugation
The molecular probes IAEDANS and ATTO465 were dissolved in DMSO as a polar solvent at the concentration of 20 mM. To perform the conjugation, 30 x 10^{-9} moles of EST2-S35C in 25 mM Tris/HCl buffer at pH 7.4 containing 1 mM reducent agent TBP were incubated over-night in the dark, at room temperature, in the presence of a 10-fold molar excess of the molecular probe. At this pH value, thiol groups are sufficiently nucleophilic to react almost exclusively with the fluorescent probes, the more numerous amines on the protein surface being protonated and relatively unreactive. Upon completion of the reaction, the excess of the free probe was removed by a gel filtration column (Sephadex G-25 column) and extensive dialysis at 4°C in 25 mM Tris/HCl at pH 7.4. The protein-fluorescent probe concentration was determined using the Bio-Rad dye reagent (BIO-RAD – USA) with bovine γ-globulin as the standard, according to the Bradford method [18]. Aliquots of the conjugate EST2-S35C were functionally characterized in the absence and presence of paraoxon assaying activity, as described in standard and inhibition assays.

2.7. IAEDANS Fluorophore derivatization
Commercially available IAEDANS (Thermo Fisher) fluorophore was derivatized with β-mercaptoethanol (SIGMA) to perform control experiments. Reaction was performed in ammonium bicarbonate buffer at pH 7.0. To a freshly prepared IEDANS solution (2.0 mg/mL), a 10 molar excess of β-mercaptoethanol was added. The reaction mixture was kept at room temperature for two hours and then at 4°C overnight. The mixture was then vacuum concentrated to few microliter of oil, and precipitated with ice cold diethyl ether to remove excess of β-mercaptoethanol to give a dark brown/black powder. The product was immediately dissolved in 25 mM Tris/HCl pH 7.5 and stored at 4°C protected from light.

2.8. Cell viability testing
1x10^4 HEK293 cells/well were seeded in a 96 well plate and incubated overnight at 37 °C and 5% CO_2 in 100uL of 10 % FBS/DMEM. The cells were then treated with varying dose ranges of the EST2 protein (0.175, 0.35 and 0.7 nmol) in replicates of six for 24 hours. The cell viability was determined using the Cell Titer-Glo luminescent cell viability assay kit (Promega, Madison, WI), according to the manufacturer's instructions. The luminescence was measured using the GLOMAX 96 microplate luminometer (Promega). The data were normalized with respect to a background signal obtained in the presence of the only culture medium.

2.9. Fluorescence spectroscopy
Fluorescence spectroscopy measurements were carried out in a Horiba Jobin–Yvon Fluoromax-4 fluorimeter, equipped with a Peltier-type temperature control system, at the temperature of 30 °C, using a quartz cuvette of 1.0 cm optical path. The emission spectra of fluorescent probes, alone and conjugated with EST2-S35C, were recorded in the range from 300 to 550 nm using an excitation wavelength of 340 nm for IAEDANS and 453 nm for ATTO465, a 0.5 nm step resolution, and a 100 nm/min scan speed with 3 accumulations.
FRET experiments were performed on a reduced volume quartz cuvette with a 1.0 cm path length. Temperature of 30 °C was kept constant by the peltier unit with 3 nm slit excitation slit and 5 nm

emission slit, 0.5 nm data interval and 3 accumulation. Spectra were recorded in the 320–600 nm region and in the 400–600 nm region with excitation wavelengths of 280 and 336 nm, respectively. Fluorescence spectra were smoothed adopting a Savitzky–Golay filter with a 15 points window. Fluorophore and buffer (Tris/HCl pH 7.5) concentrations were kept constant at 1.2 μM and 25 mM, respectively. Increasing aliquots of a buffered stock solution of paraoxon were added to reach the desired fluorophore:paraoxon ratio in a 1 mL solution of either the β-mercaptoethanol-derivatized IAEDANS, the latter mixed with unlabeled EST2 S35C protein, and the labeled EST2-S35C-IAEDANS protein.
All the fluorescence measurements were in triplicate.

2.10. Flow cell set-up and Fluorescence measurements
The set-up of fluorescence measurements in a flow-system was carried out using Starna fluorimeter cells, Type 73-3-F flow cells, with a measurement volume of 100 μl and a 3 mm optical path and a Z height of 15.0. The sample solution, containing 25 mM Tris/HCl buffer, pH 7.4 and 0.9 x 10^{-6} M of labeled EST2-S35C, was circulated using a single-channel Peristaltic Pump P-1 (GE Healthcare Life Sciences - USA) at the flow rate of 1 ml/min. Approximately 1.6 mL of the sample solution was circulated and the reservoir was kept at RT in a temperature-controlled water bath. The fluorescence signal was continuously monitored at the emission wavelength of 460 nm with excitation at 340 nm for IAEDANS, and at the emission wavelength of 490 nm with excitation at 453 nm for ATTO465. At different times, aliquots of 6 or 25 μl of buffer 25 mM Tris/HCl pH 7.4, inhibitor (0.1 x 10^{-6} M), substrate (1% p-NP-exanoate) and other compounds, such as 70 % ethanol and 100 %acetonitrile, were added to the reservoir in order to measure changes in the fluorescence signals.
Bleaching-free fluorescence measurements in the flow-cell setup were carried out by recording data points every 5.5 seconds with 0.5 seconds of integration time. Shutter was closed after each data point acquisition. Slits were set to 5 nm.
The acquired spectra were imported in the ASCII format and elaborated using the Qtiplot (Copyright 2004-2009 Ion Vasilief) and Origin (© OriginLab Corporation) softwares. The locally weighted scatter-plot smoothing (LOWESS) method, that combines multiple regression models in a k-nearest-neighbor-based meta-model, was used in the elaboration of the raw data from the fluorescence measurements in a flow-system.

3. Results and Discussion

3.1. Computational analysis
The EST2 sequence contains only one cysteine residue at position 97 (Fig 1a). The analysis of the EST2 3D-structure obtained by X-ray diffraction of protein crystals [19] indicated that the single cysteine residue is buried under the protein surface and far from the catalytic site (Fig. 1b). This feature opens up the possibility of introducing a cysteine residue in another part of the protein in order to use it as a hook for the binding of a fluorescent probe. We explored all the available positions near the catalytic tunnel, starting from the evidence that the major part of the OP moiety binds to the protein in the alcohol binding pocket of the catalytic site [13]. The residue of serine 35, located in a loop near the entrance of the alcohol binding pocket and exposed on the protein surface, appeared to be functional to the substitution with a cysteine in the 3D-structure (Fig. 1b). After structure minimization of the mutated protein, carried out in an *in silico* analysis, we obtained three possible rotamers of C35 without steric collisions, the best with a favorable score of -2. The backbones of the native and mutate proteins were almost overlapping, with very slight differences in the nearby C35 side chain structural organization. Indeed, the side chain of serine 35 was so exposed on the protein surface that it was not expected to affect the protein fold. These results were used to design the new EST2 mutant.

3.2. Over-expression and purification of EST2-S35C in E. coli

An over-expression system in *E. coli* was devised as described in the experimental section. The overall final yield was 10 mg of pure protein per liter of culture, comparable to those of the wild type EST2 obtained by Manco et al. [15]. The final specific activity was 1,943±100 units/mg and was comparable with that measured for the native enzyme of 2,375±150 units/mg in the same conditions.

3.3. Biochemical characterization

EST2-S35C maintained almost unchanged the activity towards the short-chain p-NP esters, as measured in the standard enzymatic assays carried out as described in the experimental session. The kinetic constant values determined for EST2-S35C (K_M of 14.1 ± 0.8 μM and k_{cat} of 3713 ± 256 s^{-1}) are similar to the kinetic constants previously determined by using the wild type enzyme (16.8 ± 0.2 μM and 4325 ± 210 s^{-1}) [20]. In agreement with the observations of the computational analysis, these results confirmed that the catalytic site is not affected by the mutation and therefore the structure-function relationship is unchanged. Indeed, the structural analysis carried out by circular dichroism in the far-UV region indicated that the secondary structure of EST2-S35C is maintained, there being no significant changes in the far-UV spectra with respect to the wild type. Moreover, like the wild type enzyme, EST2-S35C was sensitive to the inhibition by paraoxon. The assay of the EST2-S35C residual activity after incubation with paraoxon showed that the enzyme is rapidly and irreversibly inhibited by the organophosphate, also at very low concentrations such as 0.1 x 10^{-6} M. Although the introduction of a sulfur instead of an oxygen atom on the protein surface did not affect the structure-function features of EST2, it was not so easy to predict the effects on the protein structure-function relationship after labeling with fluorescent probes. Therefore, we proceeded by measuring the catalytic efficiency of EST2-S35C conjugated with IAEDANS or with ATTO465 on p-NP esters as the substrate. The results obtained indicated that the activity remained unchanged with respect to the unbound enzyme. These findings suggest that the binding of fluorescent probes near the alcohol binding site does not affect the binding of the substrate and the function of the enzyme in the alcyl binding site. In fact, the labeled EST2-S35C, like the free enzyme, was fully inhibited by paraoxon, assessed by measuring the residual activity in standard conditions (Supplementary Fig. S1).

3.4. Fluorescence analysis

Probes specific for the binding to cysteine residues, such as IAEDANS and ATTO465, were chosen on the basis of their properties. In particular, the excitation and emission wavelengths of these probes, as well as the emission signal decay time, are relatively insensitive to pH and other environmental changes, such as temperature. These fluorophores show a high photo- and thermal stability and a relatively long fluorescence lifetime, 0.6-3.8 nanoseconds for ATTO465 and 10-15 nanoseconds for IAEDANS. Furthermore, they have a large stokes shift: Ex_{max} 453 nm and Em_{max} 508 nm for ATTO465 and Ex_{max} 340 nm and Em_{max} 435 nm for IAEDANS. The conjugated complexes EST2-S35C-ATTO465 and -IAEDANS changed their maximum of emission wavelength to 515 nm and 460 nm, respectively (Fig. 2A,B). The observed fluorescence decay times of the probes conjugated to EST2-S35C, in particular, after 180 min of exposure to the excitation wavelength of 453 nm are shown in Figs. 2C and D. The EST2-S35C-ATTO465 and the EST2-S35C-IAEDANS conjugates showed a decay of the emission spectra greater than 90 % (Fig. 2C) or 30 % (Fig. 2D), respectively. The fluorescence decay observed was principally related to a photobleaching event that affected probes continuously exposed to the excitation wavelength. In fact, the fluorescence of EST2-S35C-IAEDANS after 15 days storage at 4 °C in the dark, continued to be very high (Fig. 2D), with just a slight redshift observed and a lower efficiency of the fluorescence emitted after continuous exposure to the excitation light (Fig. 2D). Anyway, the fluorescence signal continued to be measurable for hours starting from very high intensity values. Moreover, the fluorescence signals of the EST2-S35C-IAEDANS complex were constant in the range of pH from 6 to 8.5 (Supplementary Fig. S2), also in more organic buffers such as Tris/HCl.

These results support the use of this bioreceptor in potable water (pH ranging from 6.5 to 9.5) and biological fluids, such as blood (pH ranging from 7.35 to 7.45) and urine (optimal pH ranging from 6.5 to 7.2).

3.5. Organophosphate biosensing

In scheme I, a representation of the fluorescence measurement system is reported. The flow cell was filled with a solution containing the labeled EST2-S35C and inserted in the fluorimetric apparatus representing the biorecognition element, while the reservoir acted as the connection of the system to the external environment. At a flow rate of 1 ml/min there was a good balance between the noise of the circulating solution at a higher rate (Supplementary Fig. S3a) and the time required for a complete recirculation of the sample (about 1.5 min). We verified that the labeled-protein sample was not damaged by continuous circulation for several hours by checking the enzymatic activity at different times. We monitored the fluorescence of the EST2-S35C-IAEDANS versus time at the wavelength of 460 nm, and as expected, we observed a significant decay of the signal in the first part of the measurement time (Supplementary Fig. S3b). We registered a photobleaching phenomena due to the continue exposition of fluorescent probe to the excitation light. This slowed down after several minutes before becoming stable.

The addition of paraoxon aliquots (0.1×10^{-6} M) in the external reservoir, for a final concentration of $6{,}25 \times 10^{-8}$ M, resulted in a break in the continuity of the decay signal, that restarted at a lower value and with a different slope (Fig 3). Lower concentrations became undetectable using this apparatus.

The addition of paraoxon inhibits immediately the amount of enzyme present in the reservoir, completely quenching its fluorescence (break in the signal decay). The excess of paraoxon start to diffuse in the remaining part of system stoichiometrically inhibiting the remained free enzyme and completing the fluorescence quenching (curve after break). The subsequently diffusion process diluted the inhibited enzyme (quenched) with the remained free enzyme (not-quenched) in the circuit and we observe a small recover in fluorescence.

The previous addition of the same or higher volumes of buffer to the reservoir had no effect on the fluorescence signal of the EST2-S35C-IAEDANS complex, allowing us to exclude any interference due to the small sample dilution that occurred when the inhibitor was added. Measurements carried out on samples stored for 15 days at 4 °C gave the same results. With the only difference being an increased decay in the initial part of the curve.

We studied also the effects of other substances, like organic solvents and substrates, to the capability of the EST2-S35C-IAEDANS complex to recognize paraoxon (Fig. 4). The addition of water or an organic solvent, such as ethanol or acetonitrile, had no effects on the fluorescence signals of the EST2-S35C-IAEDANS complex (insert Fig. 4). The native stability of this protein permitted us to continue the measurements, adding other substances. The addition of a substrate excess (1% p-NP-exanoate) resulted, as expected, in a temporary quenching of the fluorescence signal recovered in less than 5 min, but without a break in the signal, because of the interaction inside the catalytic site. Anyway, since the substrate was hydrolyzed by the enzyme, the catalytic site was left unchanged, so the EST2-S35C-IAEDANS complex retained its capability to recognize paraoxon. Indeed, the addition of paraoxon also in the presence of all these substances caused an irreversible and detectable change in the fluorescence signal, observable as a break in the curve (insert Fig. 4).

The flow system has been partially re-engineered to overcome some of the previously observed limitations. First, the data sampling was decreased from 1 to 0.2 s^{-1}. This allowed the shutter closure between each acquisition, thus lowering the observed photobleaching. Moreover, the data integration was increased from 0.1 to 0.5 seconds to reduce the noise. A second significant modification consisted in the inversion of the flux. This significantly increased the signal-to-noise ratio, since, with this setup, the pump-dependent diffusion could be prevented. This is demonstrated by the strong and sharp peaks observed upon addition of the fluorescent protein (Fig. 5), with the relative diffusion peaks in the 300 seconds following the protein addition.

With this apparatus, a clear and fast signal drop can be observed when paraoxon was added. The measurement of this drop can be then correlated to the amount of paraoxon in solution. The absence of enzymatic activity, measured in the standard conditions, of the EST2-S35C-IAEDANS solution recovered after florescence measurements in presence of paraoxon, confirmed the complete inhibition of the labeled enzyme. These results support the use of the EST2-S35C-IAEDANS complex as bioreceptor in an OP biosensing devices.

3.6. Specificity of EST2-S35C-IAEDANS quenching in presence of paraoxon

We used free IAEDANS derivatized by β-mercaptoethanol and BSA randomly labeled to IAEDANS (BSA-IAEDANS) in order to demonstrate the specificity of our system, and confirm that changes in the fluorescence signals are not in charges to random interactions between paraoxon and IAEDANS free or bond to a generic protein. Stern-Volmer plot of the of EST2-S35C-IAEDANS fluorescence against equivalent of paraoxon showed a saturation quenching at one equivalent of inhibitor, while a constant signal (absence of quenching) was measured in the presence of the same amount of free fluorophore and a mix of the free fluorophore and the unlabeled EST2-S35C (Fig. 6A).

In order to exclude a generic effect of the protein structure in the quenching of IAEDANS, we tested samples of BSA labeled with IAEDANS under the same experimental conditions.

The BSA protein sequence contains 35 cysteine residues as possible binding sites for the IAEDANS reactive group; therefore, the resulting reaction should be represented by a non-homogeneous sample containing different concentrations of randomly labeled-proteins. In agreement with the stability of the fluorescent signal observed for the EST2-S35C-IAEDANS complex, we observed a decay of the BSA-IAEDANS fluorescence signal, confirming the photobleaching event affecting IAEDANS due to a continued exposure to the excitation wavelength. The addition to the reservoir of small aliquots of buffer resulted in a change in the decay curve with minor effects on the curve slope (Supplementary Fig S4). The addition of the same volumes of paraoxon to the reservoir gave the same results observed for the buffer addition, supporting the evidence that the fluorescence of IAEDANS randomly bond to the BSA surface was affected only by sample dilution. Probably, the high amount of fluorescent probe exposed on the protein surface are more sensitive to changes in volumes with respect a single probe in a protein cavity like labeled EST2-S35C.

These data indicated the absence of specific interactions between the paraoxon molecules and the IAEDANS free or bonded to a generic protein, in particular free IAEDANS is not affected by the presence of paraoxon also in presence of the protein, and supported a specific and local effect of paraoxon on the fluorescence quenching of the EST2-S35C-IAEDANS complex.

3.7. EST2-S35C-IAEDANS quenching mechanism

Irradiation of EST2-S35C at 280 nm results in a strong fluorescence band centered at 335 nm (Supplementary Fig. S5A). Given such overlap with the IAEDANS absorption spectrum, FRET experiments have been performed both to test IAEDANS localization in proximity of the binding site and the mechanism of quenching.

When the IAEDANS-labeled protein was irradiated at 280 nm, a strong fluorescence in the 400-550 nm range can be measured. In contrast, when the unlabeled protein was mixed with an equal amount of free IAEDANS, no significant emission was measured in this spectral range, whereas a strong decrease of the signal at 335 nm could be measured (Supplementary Fig. S5A). The measured emission spectrum can be explained in terms of the energy transfer between the tryptophan residues of EST2 and the IAEDANS probe, and demonstrates the localization of the probe in the proximity of the paraoxon binding site. In principle, each or a combination of the four tryptophan residues can lead to the FRET signal, though W^{85} and W^{213} are at less then 2 nm from C^{35}, and both are very close to the binding site (Supplementary Fig. S6).

In a previous work, we demonstrated that W^{85} fluorescence depends on the paraoxon concentration [13]. For this reason, we measured the FRET signal in the presence of increasing amount of paraoxon. As shown in Supplementary Figure S5B, the fluorescence at 475 nm is

affected by paraoxon, whereas the fluorescence at 335 is not significantly altered by the presence of paraoxon. Since a strong quench of W^{85} had to be expected [13], the observed behavior could be explained by the assumption that the latter tryptophan is the main responsible for the energy transfer.
Three reasons can therefore explain the observed IAEDANS quench: (i) W^{85} emission is quenched by the presence of paraoxon, resulting in a lower FRET; (ii) a mutual reorientation of the fluorophores upon paraoxon binding; (iii) a different solvation state induced by the paraoxon binding. The first explanation cannot be excluded, though it does not explain the observed quenching after paraoxon addition when the IAEDANS is directly excited at 336 nm (Fig. 6B). Moreover, a change in the chemical environment is generally followed by a change in the emission maximum, confidently discarding the third mechanism. It can be thus concluded that a change in the orientation and/or in the rotational freedom of the fluorophore does occur when EST2 binds the paraoxon.

3.8. Effects of the labelled EST2 mutant in living cells

In order to support the use of this kind of bioreceptor in operative conditions, which include the analysis of potable water or organic fluids, such as urine, we tested the toxicity of labeled EST2-S35C on living cell cultures. We chose as the study system a human embryonic-kidney non-cancerous cell-line, which has been widely used as a model in a number of studies, including investigations on the effects of drugs and chemicals on living cells[21–23]. The detection is based on the luciferase reaction assay, measuring the amount of ATP from viable cells. In particular, since the amount of ATP in the cells correlates with the cell viability, we were able to determine the number of viable cells in culture. The results, obtained after 24 hours of incubation in the presence of the labeled protein (Fig. 7), indicated the absence of any toxic effects of the labeled EST2-S35C on cell viability. These findings support the safe use of this bioreceptor in biosensing devices for environmental and diagnostic use.

4. Conclusions

The detection of chemicals in the environment is mandatory, given the astonishing number of harmful compounds present, an amount which is increasing every year [24,25], and considering the fact that the effects of several of these chemicals have been found to persist with half-life of months, if not years [26–28].

As previously described, there are other data in the literature concerning the use of fluorescence-based biosensing devices for the detection of OPs, in particular, by exploiting organophosphorus hydrolase activities [29,30], sometime achieving a very sensitive LOD [31]. However, most of these systems are based on an indirect measurement of the fluorescence and still involve the use of complex solutions of at least two or three components [32]. Conversely, the system that we have developed is very singular in terms of its remarkable advantages.

In our system, we need only an EST2 molecule covalently linked to a fluorescent probe and a detection system. The fluorescent probe continuously emits fluorescence and the binding of an inhibitor such as paraoxon results in a clear signal variation, the amount of fluorescence quenching (about 15 %) depending on the protein concentration (10^{-8} M).

The fluorescence signals are not affected by dilution, as well as by the addition of solvents, such as acetonitrile or ethanol. The stability of proteins, such as EST2, to the presence of chemicals plays an important role in their use as bioreceptors. The environment represents a complex system of several chemicals dissolved in water, so a bioreceptor must have not only a high specificity, but also a high resistance to the denaturation processes mediated by organic solvents and detergents.

The direct measurement without any substrate also permits us to conceive of its use for real time-on line measurements in the field without the need for an operator. It should be very easy, and cheap, to build an automated system that exploits these features, such as a system of pump/valve in order to maintain constant the volume and the enzyme concentration permitting the continuous addition of small quantity of samples, to be applied for the monitoring of lake or river waters. Moreover, the absence of toxic effects on living cells could permit its use also in potable water pipes or in diagnostic apparatus for OP detection in blood, like glucometer for glucose determination.

The next step could be the immobilization of this complex in an optical device, such as a micro-cuvette or micro-tube, to study its efficiency in the detection of pesticides in circulating water. The use of optical fibers dipped in the solution is planned to enhance the local fluorescence of the immobilized complex as well as the development of software able to elaborate the data acquired and to return a reliable result.

The road to obtaining working biosensors for pesticides is still long, but the use of EST2-like enzymes as the bioreceptor in a biosensing device for these dangerous chemicals appears to be a good choice.

Figures

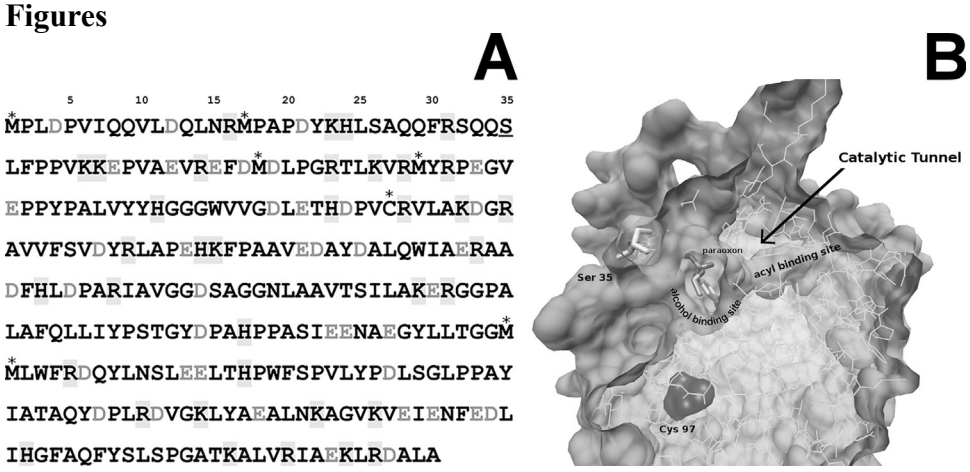

Figure 1. EST2 sequence and Structure analysis. (a) EST2 sequence in which the residues available for probe binding are highlighted, in grey the aspartic and glutamic acid residues, in grey boxes the basic residues of arginine, histidine and lysine, and with an asterisk the residues of methionine and cysteine. The residue of serine 35 is underlined. (b) Slab view of the EST2 structure with a molecule of paraoxon modeled in the alcohol binding site. The residues of serine 35 and cysteine 97 are indicated in sticks and VDW spheres, respectively. The structure image was produced by using the visual molecular dynamics (VMD) [33] software and the Tachyon built-in ray tracing engine.

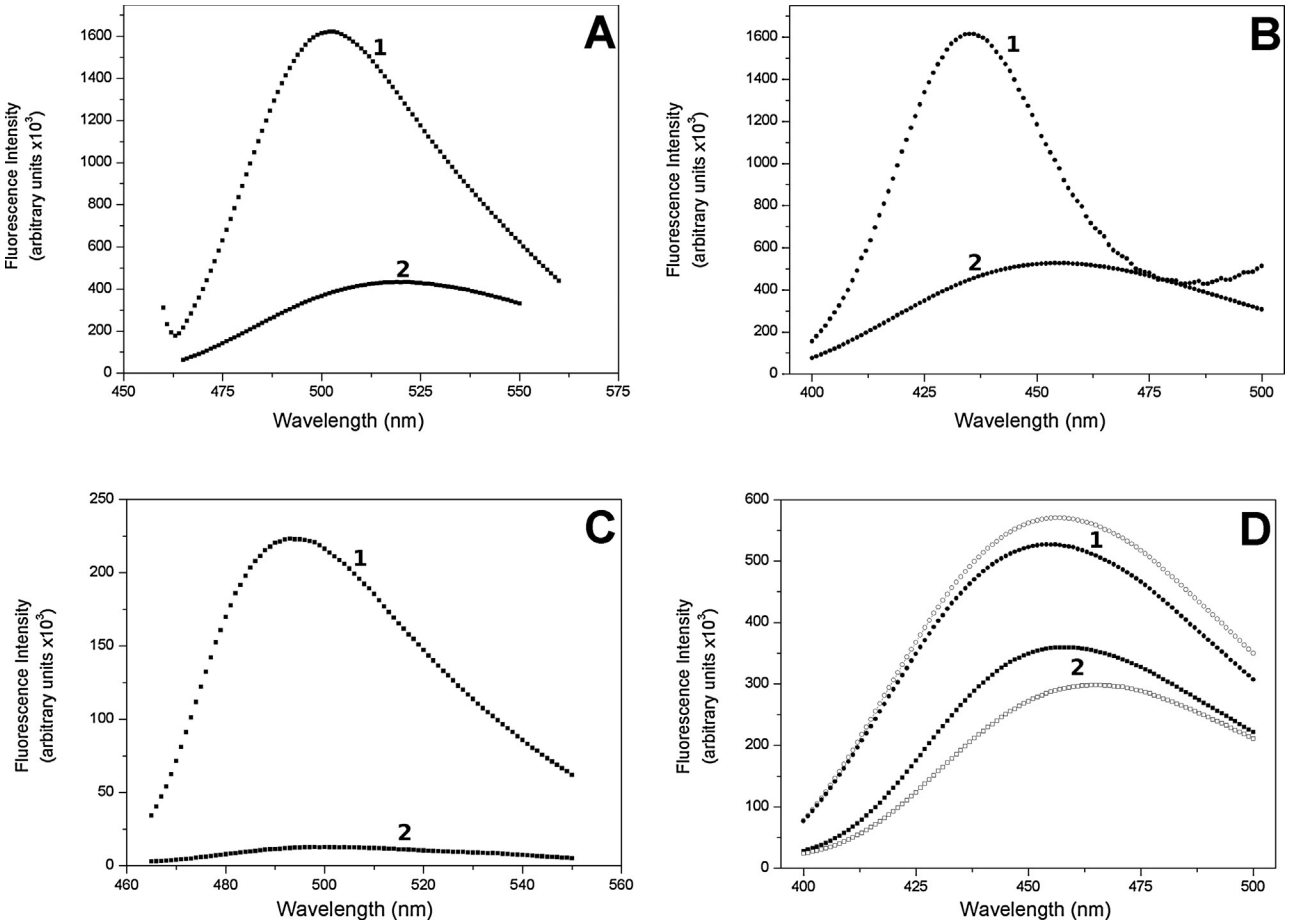

Figure 2. Fluorescence measurements of label conjugated EST2-S35C. (A) Fluorescence spectra of (1) free EST2-S35C and (2) EST2-S35C conjugated with ATTO465 at the excitation wavelength of 453 nm; (B) Fluorescence spectra of (1) free EST2-S35C and (2) EST2-S35C conjugated with IAEDANS at the excitation wavelength of 340 nm. (C) Fluorescence spectra of EST2-S35C-ATTO465 complex (1) at the start and (2) at the end of the measurement, after 180 min of continuous exposure to an excitation wavelength of 453 nm; (D) Fluorescence spectra of EST2-

S35C-IAEDANS complex (1) at the start and (2) at the end of the measurement, after 180 min of continuous exposure to an excitation wavelength of 340 nm; the sample stored for 15 days at 4 °C in the dark is indicated with open circles.

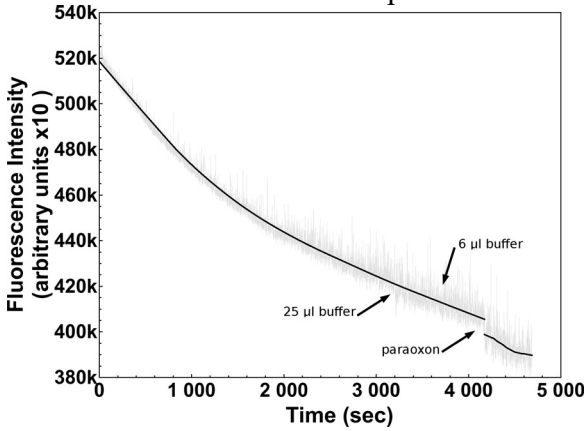

Figure 3. Flow cell fluorescence spectroscopy. Fluorescence intensity at 460 nm of the EST2-S35C-IAEDANS complex versus time. Arrows indicate the additions of buffer 25 mM Tris/HCl pH 7.4 (25 and 6 µl) and paraoxon (6 µl of 0.1 x 10^{-6} M) aliquots, at times 3180, 3660 and 4136 seconds, respectively.

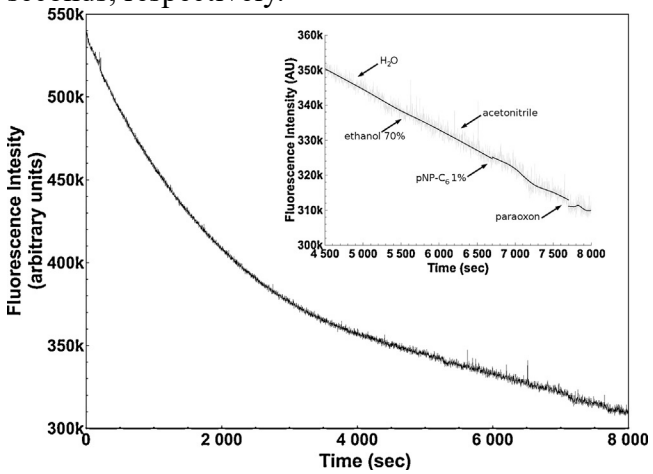

Figure 4. Effects of chemicals on EST2-S35C-IAEDANS fluorescence. Fluorescence intensity at 460 nm of the EST2-S35C-IAEDANS complex versus time. Arrows indicate the additions of the same volumes (6 µl) of H_2O at 5000 seconds, of organic solvents (70 % ethanol and 100 % acetonitrile) at 5500 and 6100 seconds, respectively, of substrate (1% p-NP-exanoate) at 6500 seconds and of paraoxon (0.1 x 10^{-6} M) at 7300 seconds.

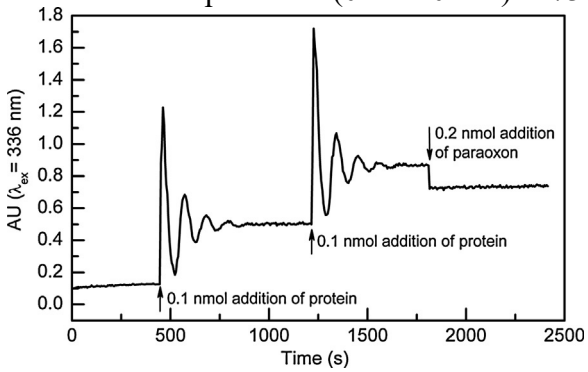

Figure 5. Fluorescence spectroscopy measurements in re-engineered flow cell. Fluorescence signal as followed against time at 336 nm excitation and 490 nm emission wavelength. When 0.1 nmol of labeled S35C mutant are added to the small 100 µL reservoir, an immediate peak can be seen. The signal slowly oscillates (~300 s) as the protein diffuses in the total volume. When 0.2 nmol of paraoxon were added an instantaneous drop of the signal could be measured.

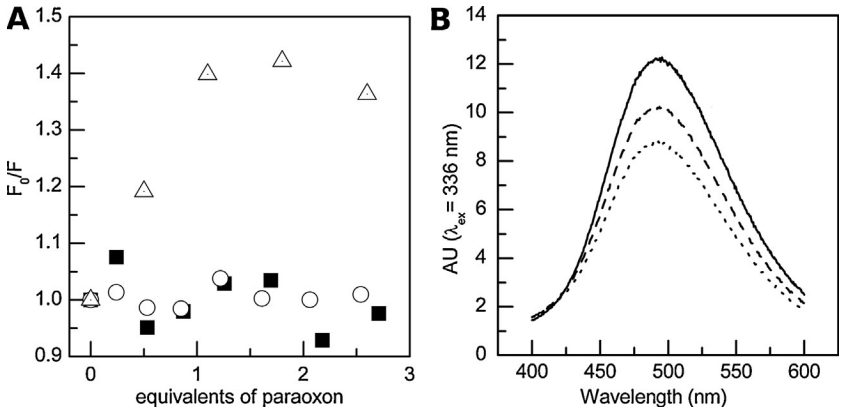

Figure 6. Effects of paroxon on the fluorescence of EST2-S35C-IAEDANS complex. (A) Stern-Volmer plot showing saturation of the quenching at one equivalent of paraoxon only for the IAEDANS labeled protein (open triangles). Control experiments, in the presence of the same amount of free fluorophore (fill squares), and a mix of the free fluorophore and the unlabeled EST2 mutant (open circle), show that signals remained unchanged. (B) Emission spectrum of EST2-S35C-IAEDANS as registered at 336 nm excitation. Addition of paraoxon equivalents induces over 25% quench of the emission signal at 490 nm.

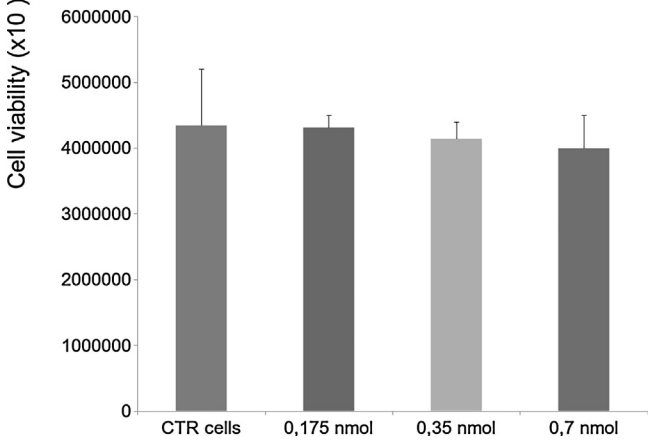

Figure 7. Cell viability testing in the presence of EST2-S35C. Viability of HEK293 cells after 24 hours incubation in the presence of increasing concentrations of EST2-S35C (0.175, 0.35 and 0.7 nmol).

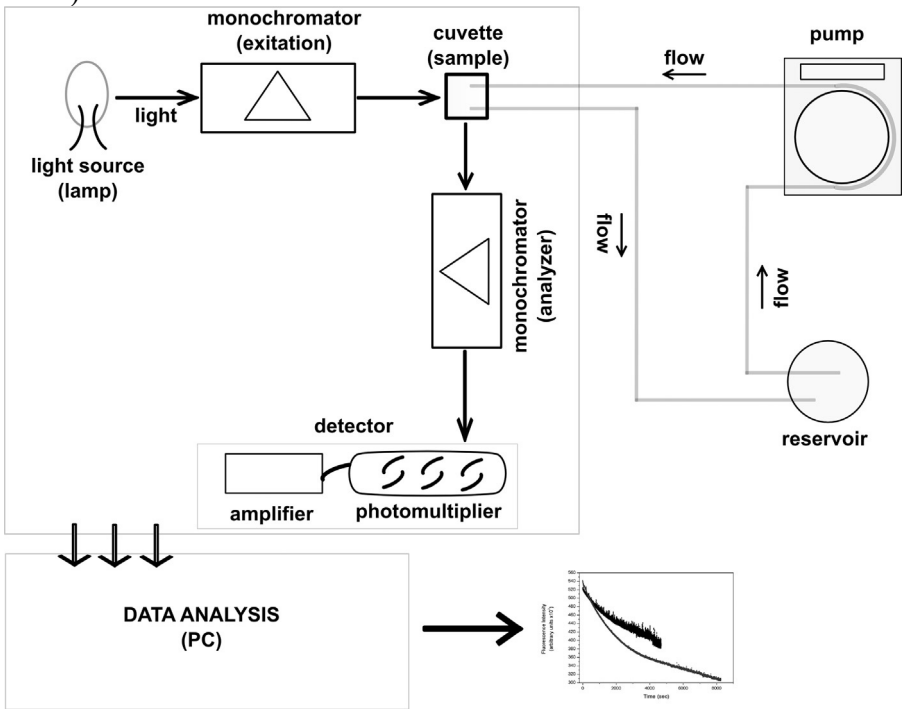

Scheme 1. Schematic representation of the flow system connected with the fluorescence

measurement apparatus and the informatics platform for the data analysis.

Acknowledgments: This work has been financed by the EU/MIUR Project PON01_01585 and PON03PE_00060_4 to G.M.
Author Contributions: P.C. and M.C. performed the fluorescence measurements, the analysis of data, the figure preparation and the writing; G.P.C. contributed to the protein expression and purification.; S.T. performed the cellular biology experiments; A.L. contributed to the analysis of fluorescence data and to the improvements of work. G.M. contributed the financial support and reviewed the manuscript; A.M. contributed to drive the cellular biology experiments and to the statistical analysis of the data, and participated in the manuscript writing; F.F. conceived and designed the experiments, performed the computational analysis, analyzed the data, and wrote the paper.

Conflicts of Interest: The authors declare that they do not have any conflict of interest.

Abbreviations

1. The following abbreviations are used in this manuscript:

EST2: Esterase 2 from *A. acidocaldarius*
EST2-S35C: Serine 35 to cysteine EST2 mutant
AchE: Acetylcholinesterases
OP: Organophosphate
Qds: Quantum dots
PL: Photoluminescent
LbL: Layer-by-layer
LOD: Limits of detection
ChO*x*: Choline oxidase
PEC: Photoelectrochemical
PON: Paraoxonase
BchE: Butyrylcholinesterase
p-NP: p-Nitrophenyl
TBP: Tri-n-butylphosphine
Paraoxon: Diethyl-p-nitrophenyl phosphate
ATTO465: ATTO 465 maleimide
IAEDANS: 5-((((2-Iodoacetyl)amino)ethyl) amino)Naphthalene-1-Sulfonic Acid
VMD: visual molecular dynamics

References

[1] J. Jeyaratnam, M. Maroni, Organophosphorous compounds, Toxicology. 91 (1994) 15–27.
[2] M. Moshiri, A. Alizadeh, M. Balali-Mood, Clinical Management of Organophosphorus Nerve Agents' Poisonings, (2014) 177–212. doi:10.1007/978-1-4471-5625-3_7.
[3] A.R.S. Iyengar, A.H. Pande, Organophosphate-Hydrolyzing Enzymes as First-Line of Defence Against Nerve Agent-Poisoning: Perspectives and the Road Ahead, Protein J. 35 (2016) 424–439. doi:10.1007/s10930-016-9686-6.
[4] G. Manco, R. Nucci, F. Febbraio, Use of esterase activities for the detection of chemical neurotoxic agents, Protein Pept. Lett. 16 (2009) 1225–1234.
[5] X. Meng, J. Wei, X. Ren, J. Ren, F. Tang, A simple and sensitive fluorescence biosensor for detection of organophosphorus pesticides using H2O2-sensitive quantum dots/bi-enzyme, Biosens. Bioelectron. 47 (2013) 402–407. doi:10.1016/j.bios.2013.03.053.
[6] N. Xia, Q. Wang, L. Liu, Nanomaterials-based optical techniques for the detection of acetylcholinesterase and pesticides, Sensors. 15 (2014) 499–514. doi:10.3390/s150100499.
[7] Z. Zheng, Y. Zhou, X. Li, S. Liu, Z. Tang, Highly-sensitive organophosphorous pesticide

biosensors based on nanostructured films of acetylcholinesterase and CdTe quantum dots, Biosens. Bioelectron. 26 (2011) 3081–3085. doi:10.1016/j.bios.2010.12.021.
[8] E.A. Songa, J.O. Okonkwo, Recent approaches to improving selectivity and sensitivity of enzyme-based biosensors for organophosphorus pesticides: A review, Talanta 155 (2016) 289-304. doi: 10.1016/j.talanta.2016.04.046.
[9] X. Li, Z. Zheng, X. Liu, S. Zhao, S. Liu, Nanostructured photoelectrochemical biosensor for highly sensitive detection of organophosphorous pesticides, Biosens. Bioelectron. 64 (2015) 1–5. doi:10.1016/j.bios.2014.08.006.
[10] F. Febbraio, S.E. D'Andrea, L. Mandrich, L. Merone, M. Rossi, R. Nucci, G. Manco, Irreversible inhibition of the thermophilic esterase EST2 from Alicyclobacillus acidocaldarius, Extrem. Life Extreme Cond. 12 (2008) 719–728. doi:10.1007/s00792-008-0179-1.
[11] D.J. Angelini, R.A. Moyer, S. Cole, K.L. Willis, J. Oyler, R.M. Dorsey, H. Salem, The pesticide metabolites paraoxon and malaoxon induce cellular death by different mechanisms in cultured human pulmonary cells, Int. J. Toxicol. 34 (2015) 433-441. doi: 10.1177/1091581815593933
[12] F. Febbraio, L. Merone, G.P. Cetrangolo, M. Rossi, R. Nucci, G. Manco, Thermostable esterase 2 from Alicyclobacillus acidocaldarius as biosensor for the detection of organophosphate pesticides, Anal. Chem. 83 (2011) 1530–1536. doi:10.1021/ac102025z.
[13] P. Carullo, G.P. Cetrangolo, L. Mandrich, G. Manco, F. Febbraio, Fluorescence spectroscopy approaches for the development of a real-time organophosphate detection system using an enzymatic sensor, Sensors. 15 (2015) 3932–3951. doi:10.3390/s150203932.
[14] N. Guex, M.C. Peitsch, SWISS-MODEL and the Swiss-PdbViewer: an environment for comparative protein modeling, Electrophoresis. 18 (1997) 2714–2723. doi:10.1002/elps.1150181505.
[15] G. Manco, E. Adinolfi, F.M. Pisani, G. Ottolina, G. Carrea, M. Rossi, Overexpression and properties of a new thermophilic and thermostable esterase from Bacillus acidocaldarius with sequence similarity to hormone-sensitive lipase subfamily, Biochem. J. 332 (Pt 1) (1998) 203–212.
[16] E. Vedejs, S.T. Diver, Tributylphosphine: a remarkable acylation catalyst, J. Am. Chem. Soc. 115 (1993) 3358–3359. doi:10.1021/ja00061a056.
[17] K. Tyagarajan, E. Pretzer, J.E. Wiktorowicz, Thiol-reactive dyes for fluorescence labeling of proteomic samples, Electrophoresis. 24 (2003) 2348–2358. doi:10.1002/elps.200305478.
[18] M.M. Bradford, A rapid and sensitive method for the quantitation of microgram quantities of protein utilizing the principle of protein-dye binding, Anal. Biochem. 72 (1976) 248–254.
[19] G. De Simone, G. Manco, S. Galdiero, A. Lombardi, M. Rossi, V. Pavone, Crystallization and preliminary X-ray diffraction studies of the carboxylesterase EST2 from Alicyclobacillus acidocaldarius, Acta Crystallogr. D Biol. Crystallogr. 55 (1999) 1348–1349. doi:10.1107/S0907444999005156
[20] L. Mandrich, V. Menchise, V. Alterio, G. De Simone, C. Pedone, M. Rossi, G. Manco, Functional and structural features of the oxyanion hole in a thermophilic esterase from *Alicyclobacillus acidocaldarius*, Proteins 71 (2008) 1721-1731. doi:10.1002/prot.21877
[21] M.-J. Lee, H.-K. Jung, M.-S. Kim, J.-H. Jang, M.-O. Sim, T.-M. Kim, H. Park, B.-K. Ahn, H.-W. Cho, J.-H. Cho, W.-S. Jung, J.-C. Kim, Acute toxicity and cytotoxicity evaluation of Dendrobium moniliforme aqueous extract in vivo and in vitro, Lab. Anim. Res. 32 (2016) 144–150. doi:10.5625/lar.2016.32.3.144.
[22] C. López, P. Zamorano, S. Teuber, M. Salas, C. Otth, M.A. Hidalgo, I. Concha, A. Zambrano, Interleukin-3 Prevents Cellular Death Induced by Oxidative Stress in HEK293 Cells, J. Cell. Biochem. (2016). doi:10.1002/jcb.25790.
[23] X. Yun, Q. Huang, W. Rao, C. Xiao, T. Zhang, Z. Mao, Z. Wan, A comparative assessment of cytotoxicity of commonly used agricultural insecticides to human and insect cells, Ecotoxicol. Environ. Saf. 137 (2017) 179–185. doi:10.1016/j.ecoenv.2016.12.002.
[24] F. Febbraio, Biochemical strategies for the detection and detoxification of toxic chemicals in

the environment, World J. Biol. Chem. 8 (2017) 13-20. doi: 10.4331/wjbc.v8.i1.13.
[25] E. Valera, R. Babington, M. Broto, S. Petanas, R. Galve, M.-P. Marco, Chapter 7 - Application of Bioassays/Biosensors for the Analysis of Pharmaceuticals in Environmental Samples, in: D.B. and S.P. Mira Petrovic (Ed.), Compr. Anal. Chem., Elsevier, 2013: pp. 195–229. doi:10.1016/B978-0-444-62657-8.00007-0.
[26] N. Bijlsma, M.M. Cohen, Environmental Chemical Assessment in Clinical Practice: Unveiling the Elephant in the Room, Int. J. Environ. Res. Public. Health. 13 (2016) 181. doi:10.3390/ijerph13020181.
[27] D. Knapton, M. Burnworth, S.J. Rowan, C. Weder, Fluorescent organometallic sensors for the detection of chemical-warfare-agent mimics, Angew. Chem. Int. Ed Engl. 45 (2006) 5825–5829. doi:10.1002/anie.200601634.
[28] A.G. Smith, S.D. Gangolli, Organochlorine chemicals in seafood: occurrence and health concerns, Food Chem. Toxicol. Int. J. Publ. Br. Ind. Biol. Res. Assoc. 40 (2002) 767–779. doi:10.1016/S0278-6915(02)00046-7.
[29] S. Paliwal, M. Wales, T. Good, J. Grimsley, J. Wild, A. Simonian, Fluorescence-based sensing of *p*-nitrophenol and *p*-nitrophenyl substituent organophosphates, Anal. Chim. Acta. 596 (2007) 9-15. doi:10.1016/j.aca.2007.05.034.
[30] L. Viveros, S. Paliwal, D. McCrae, J. Wild, A. Simonian, A fluorescence-based biosensor for the detection of organophosphate pesticides and chemical warfare agents, Sens. Actuators B Chem. 115 (2006) 150-157. doi:10.1016/j.snb.2005.08.032.
[31] R. Khaksarinejad, A. Mohsenifar, T. Rahmani-Cherati, R. Karami, M. Tabatabaei, An organophosphorus hydrolase-based biosensor for direct detection of paraoxon using silica-coated magnetic nanoparticles, Appl. Biochem. Biotechnol. 176 (2015) 359–371. doi:10.1007/s12010-015-1579-1.
[32] P. Kumar, K.-H. Kim, A. Deep, Recent advancements in sensing techniques based on functional materials for organophosphate pesticides, Biosens. Bioelectron. 70 (2015) 469–481. doi:10.1016/j.bios.2015.03.066.
[33] W. Humphrey, A. Dalke, K. Schulten, VMD: visual molecular dynamics, J. Mol. Graph. 14 (1996) 33–38, 27–28. doi:10.1016/0263-7855(96)00018-5.